Robust Estimation of the Euro-Area Natural Rate of Interest

Tino Berger[*1], Daria Kazakova[1], and Bernd Kempa [2]

[1]*University of Goettingen*

[2]*University of Muenster*

June 2022

Abstract

We set up and estimate a large-scale unobserved components model of real GDP, inflation and the real interest rate to identify the natural real interest rate of the euro area. Rather than resorting to aggregate data, we estimate a multi-country model to exploit the information contained in the national data of its 19 member countries. Our results confirm previous findings that the NRI displays a secular decline, dropping close to zero percent towards the end of the sample period. However, we find the NRI to follow a smoother path, and its decline after the Great Recession to be less sharp in comparison to previous studies. The major advantage of using our multi-country model comes in the form of a dramatic efficiency gain in estimating the euro-area NRI and a substantial improvement in the reliability of its real time performance.

JEL classification: C11, C32, E43, F33

Keywords: Natural interest rate; Euro area; Unobserved components model; Filter uncertainty

[*]Corresponding author. E-mail: tino.berger@wiwi.uni-goettingen.de

1 Introduction

The natural real interest rate (NRI) is commonly defined as the real rate consistent with a zero output gap and stable inflation. The NRI and the associated real rate gap as the difference between the actual ex-ante real interest rate and the NRI are important measures for the stance of monetary policy. Monetary policy is expansionary whenever the real short-term interest rate is below the NRI, whereas a positive real rate gap is indicative of a contractionary monetary policy stance (Wynne and Zhang, 2018). In an influential article, Laubach and Williams (2003, LW hereafter) develop a small semi-structural unobserved components (UC) model to jointly estimate the NRI, the output gap and the trend growth rate of output using quarterly U.S. data on GDP, inflation and the nominal short-term interest rate for the time period 1961Q1 to 2002Q2. They model the NRI as a time-varying process determined by the growth rate of potential output as well as other determinants reflecting (global) patterns of savings and investment. Using the Kalman filter with maximum likelihood and applying the sequential median unbiased estimator proposed by Stock and Watson (1998), LW find that both of the above factors contribute to the time variation of the NRI, although their results are subject to a substantial degree of estimation uncertainty.

Holston *et al.* (2017, HLW hereafter) re-estimate the U.S. NRI using a variant of the LW model with a longer data set by extending the sample up to the period 2016Q3. They find that the NRI has steadily declined over the past quarter century to historically low levels of close to zero. Apart from the U.S. (as well as Canada and the UK), HLW also estimate the euro-area NRI with aggregate data obtained from the Area Wide Model Database (AWM) of the European Central Bank (ECB). As with the U.S. NRI, they find evidence of a secular decline of the aggregate euro-area NRI (as well of the NRIs for Canada and the UK).[1] However, all NRIs are measured very imprecisely despite the use of longer time series compared to the original sample of LW. Beyer and Wieland (2019) confirm that estimating the U.S. NRI with the LW model is subject to a very high degree of uncertainty, but find that using AWM data for estimating the euro area NRI come with standard errors that are even larger compared to those for the U.S. NRI. Moreover, the Federal Reserve Bank of New York (FRBNY) maintains a website providing regular updates to the HLW estimates of the natural rate for the U.S., the euro area, Canada and the United Kingdom (U.K.)[2]. The current values for the euro-area NRI differ significantly from the earliest real-time estimation, at times by up to 1%. Also noteworthy is the fact that HLW suspended their real-time updates with the onset of the COVID-19 pandemic[3].

Whereas the above studies use aggregate data or estimate national NRIs, this paper is the first to develop a full-fledged multi-country model taking in all 19 countries of the euro area. Our setup adopts a model structure similar to that of HLW for each individual euro-area country. In particular, we model a common euro-area growth rate as a major determinant for the euro-area NRI. The resulting euro-area interest rate gap, i.e. the difference between the GDP-weighted ex-ante real interest rates and the euro-area NRI aligns closely with the notion of the European Central Bank's use of a euro-area Taylor rule as a benchmark for interest rate setting, in which the common NRI functions as the interest rate target (Giammarioli and Valla, 2003).

---

[1] The evidence on the euro area NRI is in line with previous estimates using variants of the LW model with AWM data, such as Mésonnier and Renne (2007) and Garnier and Wilhelmsen (2009). Common factors accounting for the decline in the NRIs of the U.S., the euro area and other countries include a slowdown in trend productivity growth, shifts in demographics, and changes in national income distributions (Rachel and Smith, 2017).

[2] See https://www.newyorkfed.org/research/policy/rstar

[3] From November 30, 2020: *Owing to the extraordinary volatility in GDP related to the COVID-19 pandemic, we are suspending until further notice the posting of regular updates of the LW and HLW model estimates.*

Previewing our results, we confirm previous findings that the NRI displays a secular decline, dropping close to zero percent towards the end of the sample period. However, we find the NRI to follow a smoother path, and its decline after the Great Recession to be less sharp in comparison to previous studies. The major advantage of using our multi-country model comes in the form of a dramatic efficiency gain in estimating the euro-area NRI and a substantial improvement in the reliability of its real time performance. Relative to a univariate model, we find the standard errors to be much lower for the multivariate model, improving the precision of estimating the NRI by a factor of up to 4. Technically, this result comes about as the use of multiple indicators reduces the filter uncertainty regarding the latent factors of the model. Whereas filter uncertainty cannot be lowered by a longer sample, a larger cross-section increases the information for estimating the latent factors. In comparison to HLW, our model also offers a substantial improvement in the reliability of its real time performance.

The remainder of the paper is structured as follows. Section 2 introduces the model, section 3 discusses our estimation approach, section 4 illustrates our results, while a final section presents some conclusions.

2 The Empirical Model

Following LW and HLW, we use a semi-structural UC model of real GDP, y_t, inflation, π_t, and the real interest rate, r_t, applied to all $N = 19$ euro area countries.

$$y_{i,t} = y_{i,t}^* + y_{i,t}^c + \varepsilon_{i,t}^y, \qquad \varepsilon_{i,t}^y \overset{iid}{\sim} \mathcal{N}(0, \sigma_{\varepsilon_i,y}^2), \quad i = 1, \ldots, N \quad (1)$$

$$\pi_{i,t} = \beta_{0,i} + \beta_{1,i}\pi_{i,t-1} + \beta_{2,i}\pi_{i,t-2,4} + \beta_{3,i}y_{i,t}^c + \varepsilon_{i,t}^\pi, \qquad \varepsilon_{i,t}^\pi \overset{iid}{\sim} \mathcal{N}(0, \sigma_{\varepsilon_i,\pi}^2). \quad (2)$$

Eq. (1) defines current output in each country as the sum of potential output $y_{i,t}^*$, the output gap $y_{i,t}^c$ and an idiosyncratic error term $\varepsilon_{i,t}^y$. Eq. (2) is a reduced-form Phillips curve, where current inflation $\pi_{i,t}$ is a function of its lagged value, inflation expectations and the output gap. Inflation expectations are approximated by $\pi_{i,t-2,4}$, i.e, the average of the second to fourth lags of past inflation.[4] Potential output follows a random walk with drift, i.e.

$$\Delta y_{i,t}^* = g_{t-1} + \eta_{i,t}^{y^*}, \qquad \eta_{i,t}^{y^*} \overset{iid}{\sim} \mathcal{N}(0, \sigma_{\eta_i,y^*}^2), \quad (3)$$

$$g_t = g_{t-1} + \eta_t^g, \qquad \eta_t^g \overset{iid}{\sim} \mathcal{N}(0, \sigma_{\eta,g}^2). \quad (4)$$

The growth rate of potential output $\Delta y_{i,t}^*$ is driven by a short-run country-specific component $\eta_{i,t}^{y^*}$ and by a long-run component g_t, where we model the latter as common to all euro-area countries. The notion of a common long-run growth rate of potential output for countries within a currency area is based on a real convergence argument in the spirit of the neoclassical growth theory. According to this argument, the removal of exchange rate risk and other barriers to trade generate capital flows to economies with lower capital-output ratios and higher marginal products of capital, thereby boosting investment and economic growth in these economies (Blanchard and Giavazzi, 2002; Tressel *et al.*, 2014).[5] We note that this way of modelling potential output does not imply the trend growth in

---

[4]This way of defining inflation expectations is similar to HLW. However, contrary to their specification, we are not imposing a unit root in the inflation dynamics as inflation rates in our sample are mean-reverting.

[5]The empirical evidence on real convergence in the euro-area since the start of the EMU is mixed. Whereas convergence has taken place in the more recent EU accession states, there is a lack of convergence among the early adopters of the euro (Franks *et al.*, 2018). However, as Diaz del Hoyo *et al.* (2017) argue, focusing the analysis on just the past two decades does not provide a sufficient understanding of the structural long-term drivers of real convergence. They find that since 1960

all euro-area countries to be identical. Rather, we decompose trend growth into a common and a country-specific component. The relative importance of these two components for each country is given by the size of $\sigma^2_{\eta_i, y^*}$ relative to $\sigma^2_{\eta, g}$ and determined by the data.

By modeling g_t as a random walk, we allow for permanent changes in the growth rate as presumably experienced during the Great Recession of 2007-09. The aggregate demand equation (5) relates the output gap in each country to its own lag as well as the lag of the common real interest rate gap $(r_t - r^*_t)$.[6]

$$y^c_{i,t} = \phi^y_i y^c_{i,t-1} + \rho_i \sum_{j=1}^{N} \Psi_{i,j,t} y^c_{j,t-1} + a_{r,i}(r_{t-1} - r^*_{t-1}) + \eta^{y^c}_{i,t} \qquad \eta^{y^c}_{i,t} \overset{iid}{\sim} \mathcal{N}(0, \sigma^2_{\eta_i, y^c}) \quad (5)$$

As in Fries *et al.* (2018), we incorporate a trade channel into the model linking the individual countries' output gaps to the GDP-weighted output gaps of the other euro-area countries.[7] Here Ψ_i denotes the time-varying GDP weights, with ρ_i measuring the strength of the trade channel for each individual country i.[8] Using weighted averages to model cross-country linkages is inspired by the Global VAR literature (see Pesaran *et al.*, 2004). The real interest rate r_t is constructed as a GDP-weighted average and common to all euro-area countries:

$$r_t = r^*_t + r^c_t + \varepsilon^r_t, \qquad\qquad \varepsilon^r_t \overset{iid}{\sim} \mathcal{N}(0, \sigma^2_{\varepsilon, r}) \qquad (6)$$

$$r^*_t = g_t + z_t, \qquad \text{with} \qquad z_t = z_{t-1} + \eta^z_t \qquad\qquad \eta^z_t \overset{iid}{\sim} \mathcal{N}(0, \sigma^2_{\eta, z}) \qquad (7)$$

$$r^c_t = \phi^r r^c_{t-1} + \eta^{r^c}_t \qquad\qquad \eta^{r^c}_t \overset{iid}{\sim} \mathcal{N}(0, \sigma^2_{\eta, r^c}) \qquad (8)$$

Eq. (6) decomposes the real interest rate of the euro area into the NRI, denoted r^*_t, the interest rate gap r^c_t and a white-noise error component ε^r_t.[9] The NRI of Eq. (7) is modeled as a function of the area's common long-run growth rate.[10] Following LW and HLW, we allow for an additional random-walk component z_t, which captures time variation of the NRI arising from other determinants impinging on the behavior of the NRI. These may include savings-investment imbalances, demographic factors or the reduction of inflation risk premia and the disappearance of intra-euro-area exchange rate risk premia since the introduction of the euro (ECB, 2004). Finally, Eq. (8) specifies a process for the evolution of the interest rate gap. Although very similar to LW and HLW, our model is closed as we include the interest rate in the observation equation (6) and model the interest rate gap in the state equation (8) as an AR(1) process.

---

there has been clear evidence of income convergence among the original euro-area member countries, although this appears to have been weakened by the Great Recession of 2007-09.

[6] The Phillips curve of Eq. (2) and the IS equation of Eq. (5) are respectively specified with single lags of inflation and the output and interest gaps in order to keep the model as parsimonious as possible. Robustness checks with alternative lag structures show that this modeling choice does not materially affect our results.

[7] Rather than analyzing a common euro-area NRI, Fries *et al.* (2018) estimate country-specific NRIs for each of the four largest euro-area economies France, Germany, Italy and Spain. To this end they develop a LW-type joint model for these four economies by explicitly taking account of their high degree of economic integration in terms of both a trade channel and a productivity channel as conduits for the international transmission of shocks.

[8] The GDP weights Ψ are computed as the ratio of each individual country's GDP relative to the sum of the remaining countries' GDPs for every year of the sample starting in 2000. Countries that have become members of the euro area later than 2000 have zero weights until the year they joined.

[9] We note that the ex-ante real interest rates in the euro area differ across countries because of country-specific inflation expectations.

[10] Eq. (7) incorporates a one-for-one relationship between the trend growth rate of output and the NRI, corresponding to a unitary intertemporal elasticity of substitution in consumption. LW have estimated this relationship and found a coefficient of close to unity. Because this relationship is not well identified in the data, we follow HLW and impose a coefficient of unity. This specification is also in line with theory. For example, Galí and Monacelli (2008) lay out a model of optimal monetary and fiscal policy in a currency union, in which the common NRI is a linear function of the trend growth rate of output across the union with a unitary coefficient.

3 Estimation approach

3.1 State space representation of the model

The model outlined by Eqs. (1)-(8) can be cast into a linear Gaussian state space model of the following general form[11]

$$\omega_t = B\alpha_t + A\kappa_t + \varepsilon_t, \qquad\qquad \varepsilon_t \sim \mathcal{N}(0, H), \qquad\qquad (9)$$

$$\alpha_t = \mu + D\alpha_{t-1} + \eta_t, \qquad\qquad \eta_t \sim \mathcal{N}(0, Q), \qquad\qquad (10)$$

where ω_t is a $p \times 1$ vector of p observed endogenous variables, modeled in the observation equation (9), κ_t is a $k \times 1$ vector of k observed exogenous or predetermined variables and α_t is a $m \times 1$ vector of m unobserved states, modeled in the state equation (10). The vectors ε_t and η_t are assumed to hold mutually independent Gaussian error terms with the former representing measurement errors and the latter structural shocks. For given parameter matrices B, A, D, μ, H, and Q, the unobserved state vector α_t can be identified from the observations $\omega_1, \ldots, \omega_T$ and $\kappa_1, \ldots, \kappa_T$ using the Kalman filter and smoother. In practice these matrices generally depend on elements of an unknown parameter vector ψ. One possible approach is to derive the log-likelihood function for the model under study from the Kalman filter (see e.g. De Jong, 1991; Koopman and Durbin, 2000; Durbin and Koopman, 2012) and replace the unknown parameter vector ψ by its maximum likelihood (ML) estimate. This is not the approach pursued in this paper. First, the large number of unobserved states as well as unknown parameters makes the maximization of the log-likelihood function quite tedious. Second, the ML estimator is subject to the so-called pile-up problem, stating that the ML estimator for the variance of time-varying parameters can be biased downwards. The exact specification of the state space form is provided in the Appendix.

3.2 Bayesian estimation

We analyze the state space model from a Bayesian point of view, i.e. we use prior information to down-weight the likelihood function in regions of the parameter space that are inconsistent with out-of-sample information and/or in which the structural model is not interpretable (Schorfheide, 2008). More formally, we treat ψ as a random parameter vector with a known prior density $p(\psi)$ and estimate the posterior densities $p(\psi \mid z_t, \kappa_t)$ for the parameter vector ψ and $p(\widehat{\alpha}_t \mid z_t, \kappa_t)$ for the smoothed state vector $\widehat{\alpha}_t$, by combining information contained in $p(\psi)$ and the sample data. Specifically, we use the Gibbs sampler to simulate draws from the joint and marginal posterior distributions of the unknown parameters and the unobserved states using conditional distributions. Intuitively, this amounts to reducing the high-dimensional model into a sequence of blocks for subsets of parameters conditional on the other blocks in the sequence.

A major advantage of the Bayesian approach to the model outlined here is that the pile-up problem can be handled by means of one-step estimation of states and parameters. The pile-up problem states that the maximum likelihood estimator for the variance of time-varying parameters has large point mass at zero, particularly if the true but unknown value is close to zero. To deal with this problem, HLW, among others, employ the Median Unbiased Estimator (MUE) developed by Stock and Watson (1998). This sequential estimation approach is based on parameter stability

---

[11]See e.g. Durbin and Koopman (2012) for an extensive overview of state space models.

test statistics, computed under the null hypothesis of constant parameter values.[12] A drawback of this approach is that analyzing uncertainty of the unobserved components, such as the NRI, becomes more complicated due to the fact that in the final estimation step a number of important parameters are imposed rather than estimated. Also, as demonstrated by Buncic (2021), HLW's implementation of Stock and Watson's MUE is unsound as it cannot recover λ_z required for the estimation of the full structural model. This suggests that the model is far from robust and therefore inappropriate for use in policy analysis. In contrast, as shown by Kim and Kim (2022), the Bayesian approach does not suffer from the pile-up problem, even with uninformative priors. The reason is that these two approaches are dealing with nuisance parameters differently. Integrating out nuisance parameters within Bayesian estimation works substantially better than maximizing out nuisance parameters as done by the maximum likelihood estimator.[13]

Moreover, the Bayesian approach yields the entire distribution of the NRI taking into account both parameter and filter uncertainty, and is thus better suited for analyzing uncertainty around the NRI.

3.3 Priors

Prior information on the unknown parameter vector is included in the analysis by way of the prior density. The prior distribution is assumed to be conditionally Gaussian for all slope parameters. For the variance parameters we use the standard inverse gamma distribution $\mathcal{IG}(c_0, C_0)$, where the shape parameter, $c_0 = \nu_0 T$, and the scale parameter, $C_0 = s_0 \sigma_0^2$, are calculated from the *prior belief* about the variance parameter, σ_0^2, and the *prior strength*, ν_0, which is expressed as a fraction of the sample size T.[14] As stated above, the main motivation for setting these priors is to down-weight the likelihood function in regions of the parameter space that are inconsistent with out-of-sample information and/or in which the structural model is not interpretable. Previous estimates as well as economic theory give us an idea about the approximate value of the model's parameters. However, using previous studies to set priors should be done with caution particularly if these studies consider the same time period. We therefore use previous estimates only as a rough indication for the prior means but choose the prior variance fairly loose. Details on the prior distributions are shown in Table 2.

3.4 Gibbs sampling scheme

The posterior density of interest is $f(\alpha, \psi | \omega)$. Given an arbitrary set of starting values $(\alpha_{\{0\}}, \psi_{\{0\}})$:

1. Block states

   Sample $\alpha_{\{1\}}$ from $f(\alpha | \omega, \psi_{\{0\}})$ according to observation equation (9) and state equation (10).

2. Block parameters

   Sample $\psi_{\{1\}}$ from $f(\psi | \omega, \alpha_{\{1\}})$

Sampling from these blocks can then be iterated J times and, after a sufficiently long burn-in period B, the sequence of draws $(B+1, ..., J)$ approximates a sample from the virtual posterior distribution $f(\alpha, \psi | \omega)$. Details on the exact implementation of each of the blocks can be found in the Appendix.

---

[12]Specifically, LW and HLW use a three-step estimation approach. By considering smaller versions of the models, in a first step they determine the signal-to-noise ratio $\lambda_g = \frac{\sigma_{\eta,g}}{\sigma_{\eta,y^*}}$, in a second step they obtain $\lambda_z = \frac{a_r \sigma_{\eta,z}}{\sigma_{\eta,y^c}}$ and in a third step they impose these two ratios in the estimation of the final model.

[13]We refer to Kim and Kim (2022) for details.

[14]Since this prior is conjugate, $\nu_0 T$ can be interpreted as the number of fictitious observations used to construct the prior belief σ_0^2.

4 Results

4.1 Data

This section presents results obtained from the multivariate model using disaggregated data for all 19 euro-area countries. Our sample extends from 2000Q1 to 2021Q2. The data is gathered from the Statistical Data Warehouse (SDW) of the European Central Bank (ECB) in the form of the country-specific gross domestic product at constant prices (real GDP), the non-energy harmonized index of consumer prices (core HCPI), and the 3-months Euro Interbank Offered Rate (Euribor). Output is a seasonally-adjusted log real GDP multiplied by 100. We seasonally adjust the core HCPI using the Census X-13 method, developed jointly by the Census Bureau and the Bank of Spain, and then use it to construct inflation and inflation expectations as well as a real effective ex-ante interest rate. Inflation expectations are approximated with a four-quarter moving average of past inflation.[15] Effective short-term interest rates are based on the Euribor and expressed on a 365-day annualized basis[16]. Then these data sequences are GDP-weighted to achieve a euro-area-wide real interest rate. For countries joining the euro area after the beginning of our sample, we use country-specific 3-month interbank rates for the respective period prior to their accession.

4.2 Euro-area NRI

Fig. 1 provides a visual comparison of our multivariate model with the corresponding estimate of HLW for the euro-area NRI and its determinants. The figure reports the posterior means of the one-sided estimates from our model (in red) and from HLW (in blue), as well as the real interest rate (in black). As becomes apparent from panels (a)-(c), the dynamics of the NRI and its components g and z are very similar in both models. The NRI follows a marked secular downward trend, reaching historic lows of around zero percent towards the end of the sample period.

Figure 1: Euro-area NRI and its components

(a) NRI   (b) z component   (c) trend growth
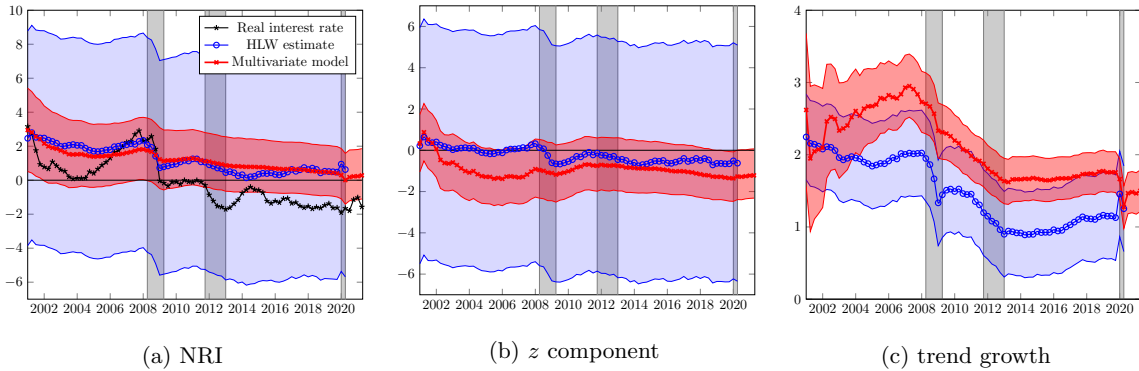
Note: Reported in red are the posterior means of the one-sided estimates, as well as the corresponding 5th and 95th percentiles. The blue shaded area shows twice the standard deviation of the NRI as estimated by HLW. The grey shaded area displays recessions in the euro-area as defined by the CEPR.

One notable difference concerns the size of the estimated decline of the NRI during the financial crisis of 2008-09, which is less dramatic in our model compared to HLW. Due to our estimate being significantly smoother, the decrease occurs gradually from 1.8% in 2008Q1 to 1.13% in 2009Q2, while the findings of HLW show a drop from 2.35% to 0.73% in 2009Q1. It is also worth mentioning that the

---

[15]This way of constructing inflation expectations is similar to HLW, whereas LW use an AR(3) model over the past 40 quarters instead. We follow HLW rather than LW in order to have as many observations for estimation as possible.

[16]Specifically, $i_t^{eff} = 100 \left((1 + i_t/36000)^{365} - 1 \right)$, where i_t is the Euribor.

NRI from the HLW model reaches a minimum of 0.14% in 2014Q2, while our estimated value declines steadily over the subsequent 10 years and dropping to 0.006% during the COVID-19 recession. The increase of the HLW NRI during the pandemic can generally be attributed to an extreme decline in the estimated output gap, which is partially offset by a respective rise in the trend-growth component g, thus driving up the NRI.

Figure 2: Interest rate gap and output gap

(a) interest rate gap
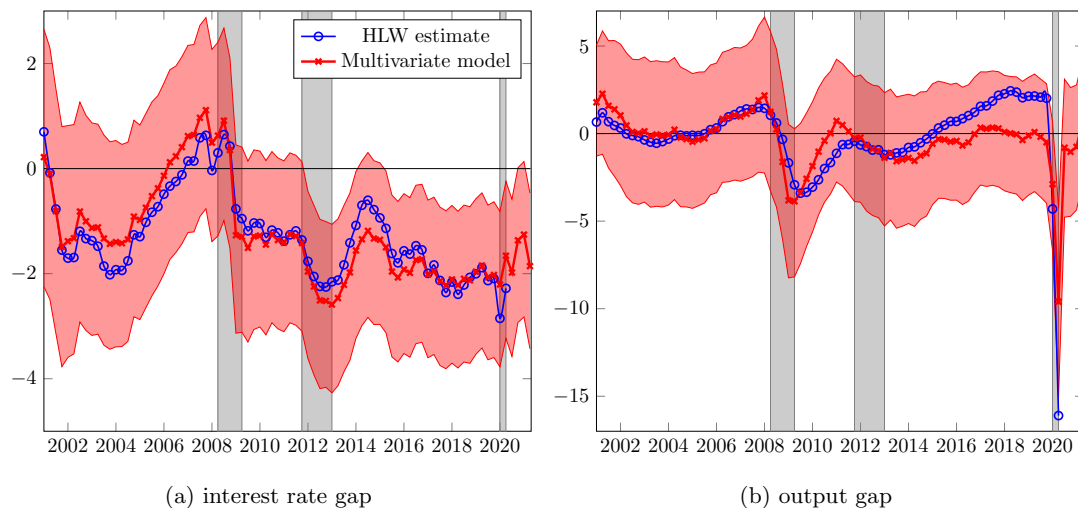
(b) output gap

Note: Reported are the posterior means of the one-sided estimates, as well as the corresponding 5th and the 95th percentiles. The interest rate gap is the difference between the real interest rate and the NRI. The output gap is the GDP-weighted average of the individual countries' output gaps. The grey shaded area displays recessions in the euro area as defined by the CEPR.

The GDP-weighted euro-area output gap and the common interest rate gap, i.e. the difference between the ex-ante real rate and the NRI is visualized in Fig. 2. We find the values of the interest rate gap to be almost identical to those reported by HLW, while the estimated output gap differs. In particular, the drop during the Great Recession is slightly larger and more rapid. Moreover, the effects of the sovereign debt crisis seem to be more persistent, while the subsequent recovery is not as drastic. HLW find that the euro-area economy has been overheating since 2014 and up to the COVID-19 recession, while our estimation yields an output gap of approximately zero during this time period. Our results are in line with OECD (2022), which classifies 2017Q4 as a turning point from the peak and the following 10 quarters as a recession. In fact our evidence shows a slight decline in the output gap from 2017Q4 until 2018Q4.

Arguably the biggest discrepancy occurs at the start of the COVID-19 recession. The HLW model yields extreme negative values of the output gap, implying comparatively higher values for trend growth.[17] In particular, the drop in 2020Q2 comprises an output gap of -16.1% and an increase in g_t from 1.13% in 2019Q4 to 1.46% in 2020Q1 and 1.25% in 2020Q2. Our model yields an estimated output gap value of -9.6% in 2020Q2 and an additional drop in g_t from 1.76% in 2019Q4 to 1.28% in 2020Q2. These findings are in line with existing literature, for instance, Bodnár *et al.* (2020) report an annual output gap decline in 2020 of approximately 10%.

Comparing the results from the multivariate model with HLW, the major difference arises with respect to the much reduced estimation uncertainty and the plausibility of the estimate in times of large-scale recessions. We now turn to a quantitative assessment of these findings.

---

[17]HLW data is available up to 2020Q2 only, as the publication of new real-time estimates of the HLW model is currently suspended.

4.3 Real-time performance of the NRI estimate

Existing measures of the NRI are characterized by a high degree of estimation uncertainty. Both HLW and Beyer and Wieland (2019) find the natural rate estimates for the euro area to be even more imprecise than those for the U.S. In particular, HLW report standard errors of the euro-area NRI of close to 4% at the end of the sample. Beside the U.S., Beyer and Wieland use data for both Germany and the euro area. Estimating the NRI for Germany, they find standard errors persistently above 2%, and reaching a maximum of close to 8% toward the end of their sample period in 2014. They also report that the standard errors for the euro-area NRI are even larger than in the German data.

Table 1: Uncertainty of the NRI and its components

	NRI	g	z
HLW model	3.157	0.296	≈ 2.860 [18]
Multivariate model	*0.740*	*0.044*	*0.744*

Table 1 quantifies the density intervals of the NRI and its components as visualized in Fig. 1. Uncertainty is measured as the standard error of the posterior distribution (at the last observation) of the respective component of the one-sided estimate. As becomes apparent, uncertainty of the euro-area NRI is explained mostly by uncertainty of the "other determinants" component z rather than by uncertainty surrounding the area's long-run growth g.[19] These results reflect the problems of estimating z reported in other studies. In particular, HLW find z never to be significantly different from zero for the euro area, and Beyer and Wieland also report high uncertainty around z. We find a dramatic efficiency gain when estimating a model with disaggregated data. Standard errors of our multivariate model are substantially smaller compared to HLW, being about six times lower for g, and almost four times smaller for the NRI as a whole[20].

The reduced estimation uncertainty in our multivariate model results in a robust real-time performance relatively to the HLW benchmark.[21] Starting with an initial sample until 2015Q4, we re-estimate the model subsequently in each quarter. Figure 3 shows the resulting NRIs obtained in the first quarter of each year. The left panel displays the well-known property of the HLW NRI in terms of large revisions when new data become available. For example, the HLW NRI estimate of 2016 is well below zero, however the final estimate turns out positive and about one percentage point above the estimate in real time. In our multivariate model, revisions are substantially smaller. The mean absolute error between the real-time estimate and the final NRI averages 0.6% in HLW and 0.2% in the multivariate NRI estimation. In fact, most of the observed differences between the real-time and the revised estimates are the results of including the COVID-19 pandemic periods in the sample. Including the most recent data from 2020Q2 onwards results in an estimated NRI that is well above the NRIs estimated prior to the COVID-19 period. The strong influence of COVID-19-related outliers in macroeconomic modeling is discussed in Lenza and Primiceri (2022).

---

[18] As HLW do not report the standard errors for z_t, we approximate them by taking the difference between the NRI uncertainty and the g_t uncertainty. This approximation is performed under the assumption that g and z are uncorrelated. The initialization of the Kalman filter assumes no correlation, but the real values for uncertainty could be higher if these components are negatively correlated.

[19] The level of uncertainty of z in our model is larger than for the NRI as a whole. This is because g and z display a (moderate degree) of negative correlation.

[20] Mirroring our results, Basistha and Startz (2008) estimate the U.S. NAIRU using a multiple-indicator unobserved components model similar to ours, where they consider a single gap driving the dynamics of cyclical fluctuations in GDP and unemployment. In particular, they show that their 4-variable model lowers overall uncertainty by about half.

[21] Due to limited data availability, we do not use vintage data in this excercise.

Figure 3: Real-time estimation

(a) HLW NRI
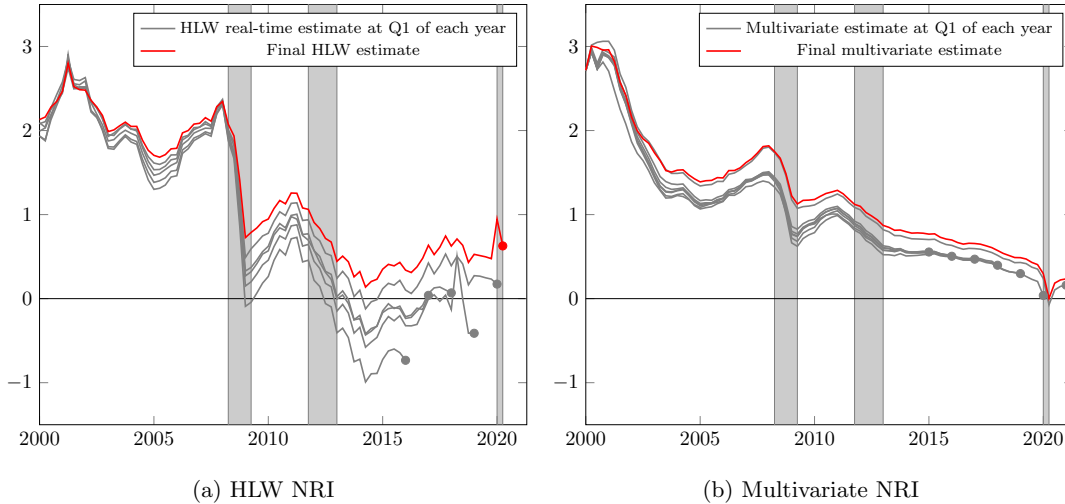
(b) Multivariate NRI

Note: Pseudo real-time estimates for the multivariate model from 2015Q1 to 2021Q2 and real-time HLW estimates from 2016Q1 to 2020Q2. The grey shaded area displays recessions in the euro area as defined by the CEPR.

Table 2 reports on the prior and posterior distributions of the model parameters[22]. The columns on the right show the mean as well as the 2.5 and the 97.5 percentiles form the posterior distribution, averaged over all countries. We take these averages at each iteration of the sampling scheme to obtain a distribution of each averaged parameter. It turns out that all parameters are (much) tighter than their prior distributions, indicating that the posterior is driven by the likelihood, i.e. by information contained in the data.

In terms of the model coefficients, we follow HLW in restricting a_r to be negative by using a truncated prior. HLW find a_r very hard to estimate with euro-area data. They state that *"For the euro-area, the slope of the IS equation is considerably flatter, and the average standard error for r^* is very large, primarily driven by draws of the parameter vector in which a_r is very close to zero and hence r^* is barely identified"* (p.S65). We obtain a similar result in which the restriction $a_r < 0$ is clearly binding and a_r has a large probability mass at values close to zero. Yet its mean is slightly more negative than that of HLW, with an average of -0.145 versus -0.037. Potentially, the inclusion of white-noise processes in equations (1) and (6) partially cover the effect of a flattening IS curve and a decreasing role of the interest rate gap in the output-gap determination in the second half of the sample.

Since we define inflation expectations as a moving average of past inflation, the sum of the coefficients β_1 and β_2 can be interpreted as a measure of inflation persistence, which is found to be significantly smaller in our model. Only for four countries, namely, Finland, Italy, Ireland and Slovenia this parameter approaches or exceeds the 0.693 mark from HLW. The slope of the Phillips Curve, β_3, is much lower in HLW than in our sample. In fact, we obtain a higher β_3 coefficient for 18 of the 19 euro-area member states, particularly so for Southern and Eastern European countries. We also find the strength of the trade channel, ρ, to be positive for almost every country, being most pronounced for Eastern Europe but turning out rather low for Northern Europe.

---

[22]Individually specified priors from section 3.3 and their respective distributions are presented in Appendix B.

Table 2: Prior and posterior distributions of model parameters

Inverse Gamma priors $\mathcal{IG}(c_0, C_0) = \mathcal{IG}(\nu_0 T, \nu_0 T \sigma_0^2)$				Posterior distribution		
σ_0^2	ν_0	2.5%	97.5%	2.5%	mean	97.5%
σ_{η_i,y^*}^2 1	0.01	0.25	602.5	2.366	2.760	3.221
σ_{η_i,y^c}^2 1	0.01	0.25	602.5	0.684	0.874	1.121
$\sigma_{\eta_r^c}^2$ 1	0.01	0.25	602.5	0.097	0.139	0.205
σ_g^2 0.05	0.01	0.01	30.1	9×10^{-6}	16×10^{-6}	31×10^{-6}
σ_z^2 0.05	0.01	0.01	30.1	4×10^{-6}	11×10^{-6}	29×10^{-6}
$\sigma_{\varepsilon_i,y}^2$ 1	0.01	0.25	602.5	0.717	0.915	1.154
$\sigma_{\varepsilon_i,\pi}^2$ 1	0.01	0.25	602.5	1.930	2.194	2.536
$\sigma_{\varepsilon_r}^2$ 1	0.01	0.25	602.5	0.030	0.048	0.079

Gaussian priors: $\mathcal{N}(a_0, A_0)$						
a_0	$\sqrt{A_0}$	2.5%	97.5%	2.5%	mean	97.5%
$\beta_{0,i}$ 1	3	-4.84	6.88	0.841	1.258	1.735
$\beta_{1,i}$ 0.5	1	-1.45	2.46	-0.040	0.046	0.135
$\beta_{2,i}$ 0.5	1	-1.45	2.46	-0.068	0.104	0.270
$\beta_{3,i}$ 0.25	0.25	-0.24	0.74	0.311	0.442	0.560
$a_{r,i}$ -0.15	0.15	-0.45	0*	-0.203	-0.145	-0.095
ϕ_i^y 0.95	0.25	0.46	0.99*	0.731	0.807	0.868
ϕ^r 0.9	0.25	0.41	0.99*	0.902	0.957	0.988
ρ_i 0.1	0.25	-0.39	0.59	0.245	0.360	0.453

Notes: Parameter from the multivariate model are country averages.
*Prior is truncated. In 4 out of 19 countries, σ_{η,y^c}^2 is set somewhat tighter to obtain robust results. See Appendix B for details.

5 Conclusion

The natural real interest rate (NRI) is a key concept in modern macroeconomics and an important tool in gauging the size of the output gap and the inflationary pressure in an economy. In fact, whether a given short-term real interest rate is inflationary or deflationary depends crucially on the level of the NRI. As an inherently unobservable variable, obtaining precise estimates of the NRI not only improves on the assessment of the state of the economy in general, but constitutes an indispensable input for informing monetary policy decisions in particular. In an influential article, Holston *et al.* (2017) provide estimates for the euro-area NRI on the basis of a small semi-structural unobserved components (UC) model using data from the Area Wide Model Database (AWM) of the European Central Bank (ECB). However, their estimates come with very large standard errors and are subject to a rather weak real-time performance.

In this paper we adopt a semi-structural modeling approach similar to Holston *et al.* (2017). Instead of resorting to aggregate data, we exploit the information contained in the country-level data of the 19 member states of the euro area. Our results confirm previous findings that the euro-area NRI displays a secular decline, dropping close to zero percent towards the end of the sample period. At the same time, we find the NRI to follow a smoother path, thereby improving the plausibility of the estimates particularly during the recessionary episodes of the financial crisis and the COVID-19

lockdowns. The major advantage of using our multi-country model comes in the form of a dramatic efficiency gain in estimating the euro-area NRI and a substantial improvement in the reliability of its real time performance.

References

BASISTHA, A. and STARTZ, R. (2008). Measuring the NAIRU with Reduced Uncertainty: A Multiple-Indicator Common-Cycle Approach. *The Review of Economics and Statistics*, **90** (4), 805–811.

BAUWENS, L., LUBRANO, M. and RICHARD, J. (1999). *Bayesian Inference in Dynamic Econometric Models*. Oxford University Press.

BEYER, R. C. and WIELAND, V. (2019). Instability, imprecision and inconsistent use of equilibrium real interest rate estimates. *Journal of International Money and Finance*, **94**, 1–14.

BLANCHARD, O. and GIAVAZZI, F. (2002). Current account deficits in the euro area: the end of the Feldstein-Horioka puzzle? *Brookings Papers on Economic Activity*, **33** (2), 147–210.

BODNÁR, K., LE ROUX, J., LOPEZ-GARCIA, P. and SZÖRFI, B. (2020). The impact of COVID-19 on potential output in the euro area. *European Central Bank Economic Bulletin 2020*, **7**, 42–61.

BUNCIC, D. (2021). Econometric issues with Laubach and Williams' estimates of the natural rate of interest. *SSRN Electronic Journal*.

DE JONG, P. (1991). The diffuse Kalman filter. *Annals of Statistics*, **19** (2), 1073–1083.

DIAZ DEL HOYO, J. L., DORRUCCI, E., HEINZ, F. F. and MUZIKAROVA, S. (2017). *Real Convergence in the Euro Area: a Long-Term Perspective*. Occasional Paper Series 203, European Central Bank.

DURBIN, J. and KOOPMAN, S. J. (2012). *Time Series Analysis by State Space Methods: Second Edition*. Oxford University Press.

ECB (2004). The natural real interest rate in the euro area. *Monthly Bulletin*, pp. 57–69.

FRANKS, J., BARKBU, B., BLAVY, R., OMAN, W. and SCHOELERMANN, H. (2018). *Economic Convergence in the Euro Area: Coming Together or Drifting Apart?*, IMF Working Paper WP/18/10.

FRIES, S., MÉSONNIER, J.-S., MOUABBI, S. and RENNE, J.-P. (2018). National natural rates of interest and the single monetary policy in the Euro Area. *Journal of Applied Econometrics*, **33** (6), 763–779.

GALÍ, J. and MONACELLI, T. (2008). Optimal monetary and fiscal policy in a currency union. *Journal of International Economics*, **76** (1), 116–132.

GARNIER, J. and WILHELMSEN, B.-R. (2009). The natural rate of interest and the output gap in the euro area: a joint estimation. *Empirical Economics*, **36** (2), 297–319.

GIAMMARIOLI, N. and VALLA, N. (2003). *The Natural Real Rate of Interest in the Euro Area*. Working Paper Series 233, European Central Bank.

HOLSTON, K., LAUBACH, T. and WILLIAMS, J. C. (2017). Measuring the natural rate of interest: International trends and determinants. *Journal of International Economics*, **108** (Supplement 1), 59–75.

Kim, C.-J. and Kim, J. (2022). Trend-cycle decompositions of real GDP revisited: classical and Bayesian perspectives on an unsolved puzzle. *Macroeconomic Dynamics*, **26** (2), 394–418.

Koopman, S. and Durbin, J. (2000). Fast filtering and smoothing for multivariate state space models. *Journal of Time Series Analysis*, **21** (3), 281–296.

Laubach, T. and Williams, J. C. (2003). Measuring the Natural Rate of Interest. *The Review of Economics and Statistics*, **85** (4), 1063–1070.

Lenza, M. and Primiceri, G. E. (2022). How to estimate a vector autoregression after March 2020. *Journal of Applied Econometrics*, **37** (4), 688–699.

Mésonnier, J.-S. and Renne, J.-P. (2007). A time-varying "natural" rate of interest for the euro area. *European Economic Review*, **51** (7), 1768–1784.

OECD (2022). *OECD Composite Leading Indicators: Reference Turning Points and Component Series*. Tech. rep., Organisation for Economic Co-operation and Development.

Pesaran, M., Schuermann, T. and Weiner, S. (2004). Modeling regional interdependencies using a global error-correcting macroeconometric model. *Journal of Business & Economic Statistics*, **22** (2), 129–162.

Rachel, L. and Smith, T. D. (2017). Are low real interest rates here to stay? *International Journal of Central Banking*, **13** (3), 1–42.

Schorfheide, F. (2008). Bayesian methods in macroeconometrics. In S. Durlauf and L. Blume (eds.), *The New Palgrave Dictionary of Economics*, vol. 1, 2nd edn., Palgrave MacMillan, pp. 402–406.

Shephard (1994). Partial non-Gaussian state space. *Biometrika*, **81** (1), 115–131.

Stock, J. H. and Watson, M. W. (1998). Median unbiased estimation of coefficient variance in a time-varying parameter model. *Journal of the American Statistical Association*, **93** (441), 349–358.

Tressel, T., Wang, S., Kang, J. S., Shambaugh, J. C., Decressin, J. and Brooks, P. K. (2014). *Adjustment in Euro Area Deficit Countries; Progress, Challenges, and Policies*. IMF Staff Discussion Notes 14/7, International Monetary Fund.

Wynne, M. and Zhang, R. (2018). Measuring the World Natural Rate of Interest. *Economic Inquiry*, **56** (1), 530–544.

Appendix A Gibbs sampling algorithm

In this appendix we provide details on the Gibbs sampling algorithm used to jointly sample the unobserved components α and the parameters ψ.

Block 1: Sampling the unobserved components α

For notational convenience, let $\tilde{y}_t = \{y_{i,t}\}_{i=1}^N$ denote $y_{i,t}$ stacked over all N countries. A similar notation is used for all observed and all latent variables. Likewise, we stack parameters over countries, i.e. $\tilde{\xi} = (\xi_1, \ldots, \xi_N)$. We first filter and draw the state vector $\alpha_t = (\tilde{y}_t^*, \tilde{y}_t^c, r_t^c, g_t, z_t)$ conditionally on the parameters ψ using the standard forward-filtering-backward-sampling approach. More specifically, using the general notation in equations (9)-(10), the state space representation is given by

$$
\overbrace{\begin{bmatrix} \tilde{y}_t \\ \tilde{\pi}_t \\ r_t \end{bmatrix}}^{\omega_t} = \overbrace{\begin{bmatrix} I_N & I_N & 0_{N,1} & 0_{N,1} & 0_{N,1} \\ 0_{N,N} & diag(\beta_3) & 0_{N,1} & 0_{N,1} & 0_{N,1} \\ 0_{1,N} & 0_{1,N} & 1 & 4 & 1 \end{bmatrix}}^{B} \overbrace{\begin{bmatrix} \tilde{y}_t^* \\ \tilde{y}_t^c \\ r_t^c \\ g_t \\ z_t \end{bmatrix}}^{\alpha_t} + \overbrace{\begin{bmatrix} 0_{N,N} & 0_{N,N} & 0_{N,N} \\ diag(\beta_0) & diag(\beta_1) & diag(\beta_2) \\ 0_{1,N} & 0_{1,N} & 0_{1,N} \end{bmatrix}}^{A} \overbrace{\begin{bmatrix} 1_{T,N} \\ \tilde{\pi}_{t-1} \\ \tilde{\pi}_{t-2,4} \end{bmatrix}}^{\kappa_t} + \overbrace{\begin{bmatrix} \tilde{\varepsilon}_t^y \\ \tilde{\varepsilon}_t^\pi \\ \varepsilon_t^r \end{bmatrix}}^{\varepsilon_t},
$$

$$\text{(A-1)}$$

with $\varepsilon_t \overset{iid}{\sim} \mathcal{N}\left(0_{2N+1,1}, I_{2N+1}\left(\tilde{\sigma}_{\varepsilon,y}^2, \tilde{\sigma}_{\varepsilon,\pi}^2, \sigma_{\varepsilon,r}^2\right)'\right)$. I_N is the identity matrix of order N, $0_{m,n}$, denote $m \times n$ matrices with all elements equal to zero. The NRI is computed as $4 \times g_t + z_t$, since g_t is the quarterly growth rate of potential output, while r_t is measured in percent per annum.

$$
\overbrace{\begin{bmatrix} \tilde{y}_t^* \\ \tilde{y}_t^c \\ r_t^c \\ g_t \\ z_t \end{bmatrix}}^{\alpha_t} = \overbrace{\begin{bmatrix} I_N & 0_{N,N} & 0_{N,1} & 1_{N,1} & 0_{N,1} \\ 0_{N,N} & \Phi_y & \tilde{a}_r & 0_{N,1} & 0_{N,1} \\ 0_{1,N} & 0_{1,N} & \phi^r & 0 & 0 \\ 0_{1,N} & 0_{1,N} & 0 & 1 & 0 \\ 0_{1,N} & 0_{1,N} & 0 & 0 & 1 \end{bmatrix}}^{D} \overbrace{\begin{bmatrix} \tilde{y}_{t-1}^* \\ \tilde{y}_{t-1}^c \\ r_{t-1}^c \\ g_{t-1} \\ z_{t-1} \end{bmatrix}}^{\alpha_{t-1}} + \overbrace{\begin{bmatrix} \tilde{\eta}_t^{y^*} \\ \tilde{\eta}_t^{y^c} \\ \eta_t^{r^c} \\ \eta_t^g \\ \eta_t^z \end{bmatrix}}^{\eta_t},
\qquad \text{(A-2)}
$$

where $\eta_t \overset{iid}{\sim} \mathcal{N}\left(0_{2N+3,1}, I_{2N+3}\left(\tilde{\sigma}_{\eta,y^*}^2, \tilde{\sigma}_{\eta,y^c}^2, \sigma_{\eta,r^c}^2, \sigma_{\eta,g}^2, \sigma_{\eta,z}^2\right)'\right)$ and $\Phi_y = \begin{pmatrix} \phi_1^y & \rho_1\Psi_{1,2} & \cdots & \rho_1\Psi_{1,N} \\ \rho_2\Psi_{2,1} & \phi_2^y & \cdots & \rho_2\Psi_{2,N} \\ \vdots & \vdots & \ddots & \vdots \\ \rho_N\Psi_{N,1} & \rho_N\Psi_{N,2} & \cdots & \phi_N^y \end{pmatrix}$.

All initial elements of the state vector α_t are assumed to follow a normal distribution, i.e. $\alpha_0 \sim \mathcal{N}(a_0, P_0)$. We initialize stationary states by drawing from their conditional stationary distribution. We set the initial value for potential output equal to the starting value of y_t with a reasonable variance of $P_0 = 5$. This corresponds to $a_0 = 0$ for y_t^c and is consistent with its initialization. For g_t, we approximate the first value as an estimated constant by regressing the first 12 values of potential output on its own lag. We also set a_0 for z_t to -1, such that the sum of g_t (annualized) and z_t resembles the HLW value for the NRI. The initial variances for these two components are $P_0 = 0.1$ and $P_0 = 1$ respectively. Sampling α_t from its conditional distribution can then be done using the multimove Gibbs sampler of Shephard (1994).

Instead of taking the entire observational vectors, we follow the univariate treatment of multivariate series approach of Koopman and Durbin (2000) in which each of the $2 \times N + 1$ variables in ω_t is brought into the analysis one at a time. This not only offers significant computational gains, but it also avoids the risk that the prediction error variance matrix becomes non-singular.

Block 2: Sampling the parameter vector ψ

In this block of the Gibbs sampler we estimate and draw the parameters ψ. Conditioning on the states α_t, these are all unknown parameters in the standard linear regression model

$$y_t = b'x_t + u_t, \qquad u_t \sim \mathcal{N}\left(0, \sigma^2\right), \tag{A-3}$$

where x_t and b are $(\ell \times 1)$ vectors. The matrix version of (A-3) is $y = Xb + u$ with obvious notations X ($T \times \ell$ matrix), y and u ($T \times 1$ vectors). We follow the approach outlined in Bauwens $et\ al.$ (1999, p. 56-61). Prior information is represented through the following normal-inverted gamma-2 density

$$\varphi\left(b, \sigma^2\right) = f_{\mathcal{NIG}}\left(b, \sigma^2 | b_0, M_0, s_0, V_0\right), \tag{A-4}$$

with the prior information being summarized by the hyperparameters $(b_0, m_0, \sigma_0^2, v_0)$. First, b_0 is the prior belief about the coefficient vector b with corresponding prior strength $M_0 = m_0 M$ such that m_0 is defined as being the prior precision proportional to the sample precision matrix $M = X'X$. Second, σ_0^2 is the prior belief about the error variance σ^2, such that $s_0 = \sigma_0^2 V_0$ is the prior belief about the residual sum of squares s with V_0 being the corresponding prior strength defined as $V_0 = v_0 T$, where v_0 is the prior degrees of freedom proportional to the sample size T.

The posterior density of b and σ^2 in the linear regression model (A-3) with prior density (A-4) is a normal-inverted gamma-2 distribution

$$\varphi\left(b, \sigma^2 | y, X\right) = f_{\mathcal{NIG}}\left(b, \sigma^2 | b_*, M_*, s_*, V_*\right), \tag{A-5}$$

with hyperparameters defined by

$$
\begin{aligned}
M_* &= M_0 + X'X, \\
b_* &= M_*^{-1}\left(M_0 b_0 + X'X\widehat{b}\right), \\
s_* &= s_0 + s + \left(b_0 - \widehat{b}\right)'\left(M_0^{-1} + \left(X'X\right)^{-1}\right)^{-1}\left(b_0 - \widehat{b}\right), \\
V_* &= V_0 + T,
\end{aligned}
$$

and $\widehat{b}$ the LS estimator for b in (A-3). Sampling b and σ^2 from the posterior distribution (A-5) can then be done separately from

$$b \sim \mathcal{N}\left(b_*, \frac{s_*}{V_* - 2}M_*^{-1}\right), \tag{A-6}$$

$$\sigma^2 \sim \mathcal{IG}_2\left(V_*, s_*\right). \tag{A-7}$$

If $X = [.]$, the posterior density in (A-5) reduces to

$$\varphi\left(\sigma^2 | y, X\right) = f_{\mathcal{IG}}\left(\sigma^2 | s_*, V_*\right), \tag{A-8}$$

with $s_* = s_0 + s$ and V_* as defined above. For common variables, we can obtain the posterior distribution of the parameter vector as follows:

- sample ϕ^r and $\sigma_{\eta_r^c}^2$ conditioning on and r_t^c from (A-6) and (A-7) respectively by using (A-5) and $y_t = r_t^c$ and $x_t = r_{t-1}^c$.

- sample $\sigma_{\eta,g}^2$ conditioning on g_t and g_{t-1} from (A-7) by using (A-8), setting $y_t = g_t - g_{t-1}$ and

$x_t = [.]$ in (A-3).

- sample $\sigma^2_{\eta,z}$ conditioning on z_t and z_{t-1} from (A-7) by using (A-8), setting $y_t = z_t - z_{t-1}$ and $x_t = [.]$ in (A-3).

- sample $\sigma^2_{\varepsilon_r}$ conditioning on r^c_t, g_t and z_t from (A-7) by using (A-8), setting $y_t = r_t - r^c_t - 4g_t - z_t$ and $x_t = [.]$ in (A-3).

For $i = 1, \ldots, N$ we follow sample parameters one by one:

- sample $\beta_{0,i}$, $\beta_{1,i}$, $\beta_{2,i}$, $\beta_{3,i}$ and $\sigma^2_{\varepsilon_i,\pi}$ conditioning on $y^c_{i,t}$ from (A-6) and (A-7) respectively by using (A-5) and $y_t = \pi_{i,t}$ as well as $x_t = [1_{T,1}, \pi_{i,t-1}, \pi_{i,t-2,4}, y^c_{i,t}]$.

- sample ϕ^y_i, ρ_i, $a_{r,i}$ and $\sigma^2_{\eta_i,y^c}$ conditioning on $y^c_{i,t}$ and $(r_t - r^*_t)$ from (A-6) and (A-7) respectively by using (A-5) and $y_t = y^c_{i,t}$ as well as $x_t = [y^c_{i,t-1}, \bar{y}^c_{t-1}, (r_{t-1} - r^*_{t-1})]$, with $\bar{y}^c_{t-1}$ denoting the weighted average of all countries' output gaps other than country i.

- sample $\sigma^2_{\varepsilon_i,y}$ conditioning on $y^c_{i,t}$ and $y^*_{i,t}$ from (A-7) by using (A-8), setting $y_t = y_{i,t} - y^*_{i,t} - y^c_{i,t}$ as well as $x_t = [.]$ in (A-3).

- sample $\sigma^2_{\eta_i,y^*}$ conditioning on $y^*_{i,t}$ and g_t from (A-7) by using (A-8), setting $y_t = y^*_{i,t} - y^*_{i,t-1} - g_{t-1}$ as well as $x_t = [.]$ in (A-3).

Appendix B   Prior parameters

Table B-1: Prior distributions which differ from the rest of the sample

Inverse Gamma priors $\mathcal{IG}(c_0, C_0) = \mathcal{IG}(\nu_0 T, \nu_0 T \sigma_0^2)$		σ_0^2	ν_0	2.5%	97.5%	Gaussian priors: $\mathcal{N}(a_0, A_0)$	a_0	$\sqrt{A_0}$	2.5%	97.5%
Germany	$\sigma^2_{\eta_i, y^c}$	0.3	1	0.24	0.39	-	-	-	-	-
Spain	$\sigma^2_{\eta_i, y^c}$	0.5	1	0.4	0.66	-	-	-	-	-
Belgium	-	-	-	-	-	ϕ_i^y	0.95	0.1	0.75	1.15
Luxembourg	-	-	-	-	-	$\beta_{3,i}$	0.25	0.1	0.05	0.45
Malta	-	-	-	-	-	$\beta_{3,i}$	0.25	0.1	0.05	0.45
						ρ_i	0.1	0.1	-0.1	0.3
Portugal	$\sigma^2_{\varepsilon_{i,y}}$	1	0.1	0.52	2.8	$\beta_{3,i}$	0.25	0.1	0.05	0.45
Italy	$\sigma^2_{\eta_i, y^c}$	0.5	1	0.4	0.66	ϕ_i^y	0.95	0.1	0.75	1.15
France	$\sigma^2_{\eta_i, y^c}$	0.5	1	0.4	0.66	ϕ_i^y	0.95	0.1	0.75	1.15
						$\beta_{3,i}$	0.25	0.1	0.05	0.45